

## Article

# Study on the Hydrochemical Characteristics and Evolution Law of Taiyuan Formation Limestone Water under the Influence of Grouting with Fly Ash Cement: A Case Study in Gubei Coal Mine of Huainan, China

Guanhong Xiao <sup>1</sup> and Haifeng Lu <sup>1,2,\*</sup>

<sup>1</sup> School of Earth and Environment, Anhui University of Science and Technology, Huainan 232001, China; xgh05331@163.com

<sup>2</sup> State Key Laboratory for Fine Exploration and Intelligent Development of Coal Resources, Beijing 100083, China

\* Correspondence: luhaifeng7571@126.com; Tel.: +86-13625547128

**Abstract:** The hydrogeological conditions of Huainan Coalfield are complex. The Taiyuan formation limestone water (Taihui water) in this area is a direct threat to the water source of the 1# coal mining floor. In order to prevent and control water disasters, Gubei Coal Mine adopted ground high-pressure grouting with fly ash cement to block the hydraulic connection between the Taiyuan formation limestone aquifer and the Ordovician limestone aquifer. However, the injected slurry will destroy the original hydrochemical balance of Taihui water and change its hydrochemical characteristics. Taking the influence area of the 2# karst collapse column in the Beiyi 1# coal mining area of Gubei Coal Mine as an example, a total of 25 Taihui water samples were collected. The hydrochemical characteristics and evolution law of Taihui water before and after grouting are studied via the multivariate statistical method. The research methods include constant index statistics, Piper diagram, correlation analysis, ion combination ratio, and saturation index analysis. The results show that after grouting, the concentrations of  $\text{Na}^+ + \text{K}^+$ ,  $\text{Ca}^{2+}$ ,  $\text{Mg}^{2+}$ , and  $\text{Cl}^-$  in Taihui water decrease, while the concentrations of  $\text{SO}_4^{2-}$  and  $\text{HCO}_3^-$  increase. The average values of PH and TDS become larger. The hydrochemical types of Taihui water are more concentrated, mainly  $\text{HCO}_3\text{-Na}$  and  $\text{Cl-Na}$ . The correlations between conventional indicators decrease. According to the analysis of ion combination ratio, dissolution, cation exchange, and pyrite oxidation mainly occur in Taihui water, and these effects are enhanced after grouting. The saturation index results show that after grouting, the saturation index of dolomite, calcite, and gypsum is significantly reduced, and the saturation index of rock salt is slightly increased. The conclusion of this study is that the hydrochemical characteristics of Taihui water are greatly affected by fly ash cement. Moreover, because fly ash cement contains a lower calcium oxide content than ordinary Portland cement, the effect of fly ash cement on the ion concentration of Taihui water and the resulting hydrogeochemical effect are significantly different. Therefore, in the treatment of mine water disasters, the hydrogeochemical evolution law affected by fly ash cement grouting should be identified.

**Keywords:** regional grouting; fly ash cement; Taiyuan formation limestone water; hydrogeochemical evolution law



**Citation:** Xiao, G.; Lu, H. Study on the Hydrochemical Characteristics and Evolution Law of Taiyuan Formation Limestone Water under the Influence of Grouting with Fly Ash Cement: A Case Study in Gubei Coal Mine of Huainan, China. *Water* **2024**, *16*, 971. <https://doi.org/10.3390/w16070971>

Academic Editor: Liliana Leticariu

Received: 6 March 2024

Revised: 20 March 2024

Accepted: 23 March 2024

Published: 27 March 2024



**Copyright:** © 2024 by the authors. Licensee MDPI, Basel, Switzerland. This article is an open access article distributed under the terms and conditions of the Creative Commons Attribution (CC BY) license (<https://creativecommons.org/licenses/by/4.0/>).

## 1. Introduction

China is one of the countries with the most serious mine water disasters in the world [1]. According to the statistics of the National Mine Safety Administration, the risk of water disaster is second only to gas explosion. At the same time, it is also the main restrictive condition for the safety and economic exploitation of coal resources in China [2]. For example, the exploitation of North-China-type coalfields is generally threatened by floor limestone aquifers. Especially with the increase in mine excavation depth, water disasters

occur from time to time [3]. In order to prevent and control mine water disasters, since the 1980s, China has begun grouting the transformation of limestone aquifer in coal seam floors. The target area is explored and injected with cement slurry through directional drilling on the ground, and the thin limestone aquifer is transformed into an aquiclude [4].

After the implementation of the grouting project in the limestone aquifer, Taihui water is mixed with the slurry precipitation water, and the conventional ion concentration will inevitably change, which further leads to the change of the hydrochemical characteristics and hydrogeochemical evolution law of Taihui water. Taking Taoyuan Coal Mine as an example, Guo Yan studied the hydrogeochemical evolution law of Taihui water affected by ordinary Portland cement grouting [5]. As we all know, due to the huge regional grouting treatment project, a lot of slurry is needed, and the economic cost of using ordinary Portland cement is high. Researchers have found that mixing fly ash into cement to make grouting materials can solve the problems of poor performance, poor material compatibility, and high cost after consolidation [6]. At the same time, the reuse of fly ash can also reduce the environmental burden. However, after the use of fly ash cement for regional grouting treatment, the influence of hydrogeochemical characteristics and the hydrogeochemical evolution law of Taihui water have not been studied.

Multivariate statistical analysis has been widely used in the study of the hydrochemical characteristics and hydrogeochemical processes of groundwater. According to the conventional ion concentration, the hydrochemical types of groundwater can be classified. With the introduction of Piper diagram [7,8] and Durov diagram [9], the hydrochemical types and ion distribution of groundwater can be more intuitively seen. Then, the source of groundwater and the hydraulic connection between different aquifers can be preliminarily judged. The methods of ion combination ratio [10–12], correlation analysis [13], principal component analysis [14], and cluster analysis [15–17] are more conducive to the analysis of groundwater hydrochemical characteristics. The hydrogeochemical evolution of groundwater is usually reflected in the change of hydrochemical components with time or space under certain influences. Therefore, the hydrogeochemical evolution of groundwater can be revealed by analyzing the hydrochemical characteristics of groundwater.

Huainan coalfield is one of the largest coal bases in China. It is located on the southern margin of the North China Plate [18]. Gubei Coal Mine is located in Panxie Mining Area of Huainan Coalfield (Figure 1a). There is a 2# karst collapse column in the Beiyi 1# coal mining area of Gubei Coal Mine. The karst collapse column is characterized by full water filling and strong water conductivity. It poses a threat to 1# coal within a certain range. The 2# karst collapse column increases the complexity of geological conditions. In particular, it has greatly changed the mine water filling conditions in the process of coal mining [19]. For this kind of karst collapse column, the water source of the water channel of the collapse column can be cut off by grouting into the karst collapse column and its influence zone [20]. Gubei Coal Mine carries out ground grouting on the affected area of 2# karst collapse column. The grouting material is fly ash cement. After the implementation of the project, the original balance of the groundwater chemical field was destroyed. At present, the research on groundwater hydrochemistry in Gubei Coal Mine mainly focuses on the identification of mine water inrush [21–24], the change of hydrochemical characteristics under mining disturbance [25], and the chemical characteristics of shallow groundwater in the subsidence area [26]. Many scholars have also studied the chemical composition characteristics and formation of groundwater in the original environment of Gubei Coal Mine [27–29]. However, there are few studies on the hydrochemical characteristics and evolution of groundwater under the influence of grouting in this study area.

This study systematically analyzed the chemical data of Taihui water before and after grouting in this area for the first time. The purpose is to (1) analyze the changes of hydrochemical characteristics of Taihui water before and after grouting with fly ash cement; (2) clarify the hydrogeochemical evolution law under the influence of grouting with fly ash cement. The significance of this study is to provide a theoretical basis for the identification of mine water inrush and the utilization of groundwater in the region, and

also to provide a reference for the hydrogeochemical study of other coal mines under the influence of grouting.

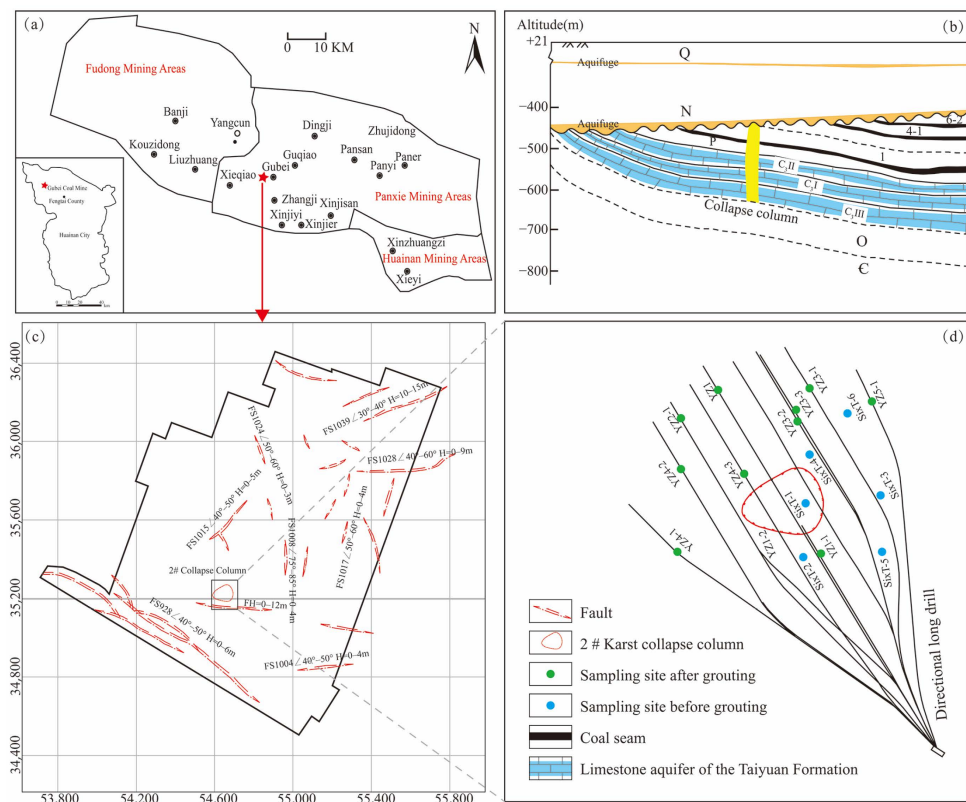


**Figure 1.** Overview of Gubei Coal Mine. (a) geographical location of study area; (b) stratum; (c) Faults and 2# karst collapse column in the study area; (d) sampling points.

## 2. Materials and Methods

### 2.1. Overview of the Study Area

Gubei Coal Mine is located in the northwest of Fengtai County, Anhui Province, adjacent to Dingji Coal Mine, and Guqiao Coal Mine. The study area belongs to the Huaihe alluvial plain, the terrain is flat, and the overall trend is high in the northwest and low in the southeast. The surface water system in the region is developed, mainly the Yongxing River and Gang River. The precipitation mainly occurred in June, July, and August, with an average annual rainfall of 926.30 mm.

The strata of Gubei Coal Mine from old to new are Cambrian, Ordovician, Carboniferous, Permian, Neogene, and Quaternary. The mining area is located in the convergence zone between the east wing of Chenqiao anticline and the west of Panji anticline. The overall structural form is a monocline structure with a north–south direction and an east-inclined direction. The stratum tilts gently, with an inclination angle of 5~15°, and there are unevenly developed secondary wide and gentle folds and faults.

According to the hydrogeological report, the main aquifer of the mine is composed of Cenozoic loose aquifer (group), Permian sandstone fissure aquifer (group), Carboniferous Taiyuan formation aquifer, and Ordovician karst fissure aquifer. The aquifers in the Cenozoic are rich in water, but because of their good aquiclude, there is no hydraulic connection between them, which has no direct impact on mine water filling. Due to the existence of geological bodies such as fault structures and karst collapse columns, the sandstone water located on the roof and floor of the coal seam is the direct water filling source of the mine. The Taiyuan formation limestone aquifer is about 18.30 m away from the 1# coal. Due to the fault and bottom plate pressure, the aquifer will become the direct source of water inflow from the 1# coal seam floor. From a regional perspective, Ordovician

limestone water can also be directly hydraulically linked to the limestone aquifer group due to faults or mining.

In the study area, a 2# karst collapse column with full water filling and strong water conductivity is developed. Its plane shape is approximately elliptical. In space, it is like a cone. The basement of the 2# karst collapse column is located in the cold ash, and the top is near the 4–1 coal. In the 2# karst collapse column, the lower part of the limestone section of the C<sub>3</sub>I group (C<sub>3</sub><sup>3under</sup>) is extremely rich in water, and the hydraulic connection between Taihui and Aohui is close. In order to eliminate the water hazard threat of 2# karst collapse column, Gubei Coal Mine implemented ground grouting treatment in the area affected by 2# karst collapse column. A total of 2 main branch holes and 17 branch holes were arranged in this grouting treatment project. The ground high-pressure grouting was carried out on the C<sub>3</sub><sup>3</sup> under and C<sub>3</sub><sup>9</sup> ash layers to change the aquifer into an aquiclude. At the same time, the hydraulic connection inside the limestone aquifers of C<sub>3</sub>I and C<sub>3</sub>II groups was blocked, and the hydraulic connection between the Taiyuan limestone aquifer and the Ordovician limestone aquifer was also blocked. The project uses a total of 329581.14 m<sup>3</sup> of fly ash cement (cement 179,424.13 t and fly ash 597.76 t). The grouting treatment project started in March 2019 and ended in September 2020.

## 2.2. Sample Collection and Processing

A total of 25 limestone water samples were collected, including 12 water samples from limestone drainage holes before grouting and 13 water samples from underground exploration verification holes after grouting. The sampling sites are in the affected area of the 2# karst collapse column (grouting treatment area) of Gubei Coal Mine, as shown in Figure 1d. The water samples before grouting were collected from July 2015 to October 2015. The water sample collection time after grouting is from January 2023 to April 2023. The groundwater samples were put into clean numbered polyethylene bottles and sent to the laboratory of the Exploration Research Institute of Anhui Province Bureau of Coal Geology. After that, each water sample was filtered with a 0.45 µm membrane and stored at 4 °C. The concentrations of conventional ions (Na<sup>+</sup>, Ca<sup>2+</sup>, Mg<sup>2+</sup>, Cl<sup>-</sup>, SO<sub>4</sub><sup>2-</sup> and HCO<sub>3</sub><sup>-</sup>), PH and TDS were measured. PH and TDS of water samples were tested on site using a multi-parameter water quality measuring instrument (BDR8100A, BELL Analytical Instruments Co., Ltd., Dalian, China). The concentration of HCO<sub>3</sub><sup>-</sup> was tested via acid–base titration. The concentrations of other ions were tested via ion chromatography (Aquion, Thermo Fischer Scientific, Waltham, MA, USA). After calculation, the cation–anion balance error of each group of data is within ±10%.

## 2.3. Analytical Research Methods

Conventional ion concentration data analysis, hydrochemical type analysis, and correlation analysis were completed by SPSS 25.0 and plotted with Origin 10.0. Saturation index analysis was performed by Phreeqc 3.7.3.

# 3. Results and Discussion

## 3.1. Characteristics of Conventional Indicators

The statistics and analysis of conventional ions, TDS, and PH in the samples can help to understand the hydrochemical characteristics of the groundwater in the coal mine [30]. In order to compare the changes of hydrochemical characteristics of Taihui water in Gubei Coal Mine before and after grouting, we count and analyze the conventional indexes of Taihui water (Table 1). Before grouting, the PH value was 8.04–8.96, with an average of 8.56. After grouting, the PH value is 8.02–10.13, with an average of 8.96, and the alkalinity of Taihui water is enhanced. Before and after grouting, the TDS values are 314.00–2845.00 mg/L and 1769.00–2514.00 mg/L. The main ions were Na<sup>+</sup>+K<sup>+</sup>, Ca<sup>2+</sup>, Mg<sup>2+</sup>, Cl<sup>-</sup>, SO<sub>4</sub><sup>2-</sup>, and HCO<sub>3</sub><sup>-</sup>. Before grouting, the values of these indexes are 51.02–1057.29 mg/L, 36.87–76.95 mg/L, 14.59–17.50 mg/L, 29.97–1109.59 mg/L, 32.80–528.33 mg/L, and 201.37–469.85 mg/L; after grouting, the values of these indexes are 676.26–947.39 mg/L, 3.21–36.87 mg/L,

0.97~12.64 mg/L, 195.96~928.79 mg/L, 88.38~557.15 mg/L, and 6.10~1293.62 mg/L. The coefficient of variation is usually used to describe the degree of dispersion of the data. In the field of groundwater, it represents the intensity of ion changes [31]. In this study, the coefficients of variation of  $\text{Ca}^{2+}$ ,  $\text{Mg}^{2+}$ ,  $\text{SO}_4^{2-}$ , and  $\text{HCO}_3^-$  were higher, and the coefficient of variation of  $\text{HCO}_3^-$  was the highest at 0.81. The higher coefficient of variation indicates that these ions may be greatly affected by grouting treatment. In addition, it also represents the key hydrogeochemical changes in Taiyuan aquifer after grouting.

**Table 1.** Statistics of conventional indicators before and after grouting.

Project		$\text{Na}^+ + \text{K}^+$ ( $\text{mg}\cdot\text{L}^{-1}$ )	$\text{Ca}^{2+}$ ( $\text{mg}\cdot\text{L}^{-1}$ )	$\text{Mg}^{2+}$ ( $\text{mg}\cdot\text{L}^{-1}$ )	$\text{Cl}^-$ ( $\text{mg}\cdot\text{L}^{-1}$ )	$\text{SO}_4^{2-}$ ( $\text{mg}\cdot\text{L}^{-1}$ )	$\text{HCO}_3^-$ ( $\text{mg}\cdot\text{L}^{-1}$ )	TDS ( $\text{mg}\cdot\text{L}^{-1}$ )	PH
Before	Minimum	51.02	36.87	14.59	29.97	32.80	201.37	314.00	8.04
	Mean	709.72	44.49	15.84	766.17	215.82	318.46	1946.17	8.56
	Maximum	1057.92	76.95	17.50	1109.59	528.33	469.85	2845.00	8.96
	Standard Deviation	361.59	10.49	0.94	413.65	139.26	72.26	874.78	0.29
	Coefficient of Variation	0.51	0.24	0.06	0.54	0.65	0.23	0.45	0.03
	After	Minimum	676.26	3.21	0.97	195.96	88.38	6.10	1769.00
Mean		818.16	18.25	6.80	632.18	280.50	473.72	2080.31	8.96
Maximum		947.39	36.87	12.64	928.79	557.15	1293.62	2514.00	10.13
Standard Deviation		72.09	9.17	3.66	182.78	174.17	383.40	189.23	0.71
Coefficient of Variation		0.09	0.50	0.54	0.29	0.62	0.81	0.09	0.08

The box plot diagram can directly reflect the changes and overall distribution characteristics of ion concentration, TDS, and PH before and after grouting [32]. According to Table 1, the box plot is drawn using Origin 10.0. From Figure 2, we can see the distribution and changes of ion concentration, TDS, and PH in Taihui water. On the whole, whether before or after grouting, the average order of the mass concentration of anion and cation in Taihui water has not changed.  $\text{Na}^+ + \text{K}^+$  is the main cation, and the mass concentration relationship is  $\text{Na}^+ + \text{K}^+ > \text{Ca}^{2+} > \text{Mg}^{2+}$ .  $\text{Cl}^-$  is the main anion, and the mass concentration relationship is  $\text{Cl}^- > \text{HCO}_3^- > \text{SO}_4^{2-}$ . The order of the average mass concentration of anion and cation does not change, but the specific numerical distribution changes. The mass concentration of cations in Taihui water after grouting decreases. The maximum value of  $\text{Mg}^{2+}$  mass concentration after grouting is less than the minimum value before grouting. The maximum value of  $\text{Ca}^{2+}$  mass concentration after grouting is the same as the minimum value before grouting. The mass concentration of  $\text{Cl}^-$  decreases, while the mass concentration of  $\text{SO}_4^{2-}$  and  $\text{HCO}_3^-$  increases. The TDS value increases, which is medium salinity water. Obviously, this further shows that grouting treatment has an impact on Taihui water.

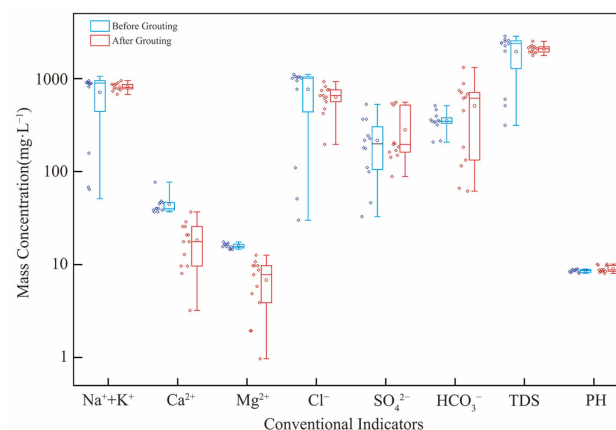


**Figure 2.** Box plot of conventional indicators.

### 3.2. Hydrochemistry Type

The piper diagram is a simple method for judging the type of water chemistry based on ion composition. It can be used to count the concentration of the main anions and cations in groundwater and explore their sources [33,34]. It can be seen from Figure 3 that before grouting, the 12 samples in the study area are divided into three hydrochemical types, of which 8.33% of the water samples are mixed, 16.67% of the water samples are  $\text{HCO}_3\text{-Mg}$ , and 75% of the water samples are  $\text{Cl-Na}$ . After grouting, the 13 water samples are divided into two types. The proportion of  $\text{HCO}_3\text{-Na}$  is 15.38%, and the proportion of  $\text{Cl-Na}$  is 84.62%. It is speculated that the hydraulic connection in the area may be weakened due to grouting, so the type of water sample is more concentrated after grouting. From the distribution characteristics of cations, the water samples before and after grouting are mainly dominated by  $\text{Na}^+$ , and the distribution of water samples after grouting is more concentrated. The distribution of anions is more dispersed,  $\text{Cl}^-$  in the water sample before grouting is absolutely dominant, and a small part is dominated by  $\text{HCO}_3^-$ . The water samples after grouting are more mixed. Without considering the chemical reaction, because the main chemical composition of fly ash cement used in grouting is calcium oxide ( $\text{CaO}$ ), silicon dioxide ( $\text{SiO}_2$ ), aluminum oxide ( $\text{Al}_2\text{O}_3$ ), iron oxide ( $\text{Fe}_2\text{O}_3$ ), sodium oxide ( $\text{Na}_2\text{O}$ ), and so on, the concentration of  $\text{Na}^+$ ,  $\text{Ca}^{2+}$ , and  $\text{SO}_4^{2-}$  in Taihui water should be increased due to the influence of grouting water. However, according to the conventional index and hydrochemical type analysis of Taihui water, in fact, the change of ion concentration and proportion in Taihui water after grouting is not only directly affected by the precipitation water of grouting but also indirectly affected by chemical reactions. During this period, the ion concentration and pH value changed due to grouting, thus breaking the original chemical reaction law. This will be analyzed in detail via the ion combination ratio.

### 3.3. Correlation Analysis

In the study of hydrogeochemistry, it is generally believed that a higher correlation represents a similar source. In this correlation analysis, seven indicators were selected:  $\text{Na}^+$ ,  $\text{Ca}^{2+}$ ,  $\text{Mg}^{2+}$ ,  $\text{Cl}^-$ ,  $\text{SO}_4^{2-}$ ,  $\text{HCO}_3^-$ , and TDS. First, the normal distribution test is carried out on the seven indicators. The results showed that there were three indicators of Shapiro–Wilk (S-W) significance less than 0.05. Obviously, this does not conform to the normal distribution [35,36]. Spearman correlation analysis was performed on the data using SPSS 25.0, and the results are shown in Table 2.

**Table 2.** Correlation coefficient matrix of water chemical composition index.

		$\text{Na}^+$	$\text{Ca}^{2+}$	$\text{Mg}^{2+}$	$\text{Cl}^-$	$\text{SO}_4^{2-}$	$\text{HCO}_3^-$	TDS
Before	$\text{Na}^+$	1						
	$\text{Ca}^{2+}$	−0.283	1					
	$\text{Mg}^{2+}$	0.383	−0.527	1				
	$\text{Cl}^-$	0.746	−0.053	0.085	1			
	$\text{SO}_4^{2-}$	0.851	−0.537	0.432	0.468	1		
	$\text{HCO}_3^-$	0.462	−0.280	−0.045	0.265	0.496	1	
	TDS	0.951	−0.223	0.332	0.764	0.816	0.406	1
After	$\text{Na}^+$	1						
	$\text{Ca}^{2+}$	0.254	1					
	$\text{Mg}^{2+}$	−0.271	0.355	1				
	$\text{Cl}^-$	0.538	0.016	−0.169	1			
	$\text{SO}_4^{2-}$	0.047	−0.017	−0.533	0.008	1		
	$\text{HCO}_3^-$	−0.041	0.213	0.528	−0.316	−0.704	1	
	TDS	0.962	0.155	−0.393	0.538	0.245	−0.217	1

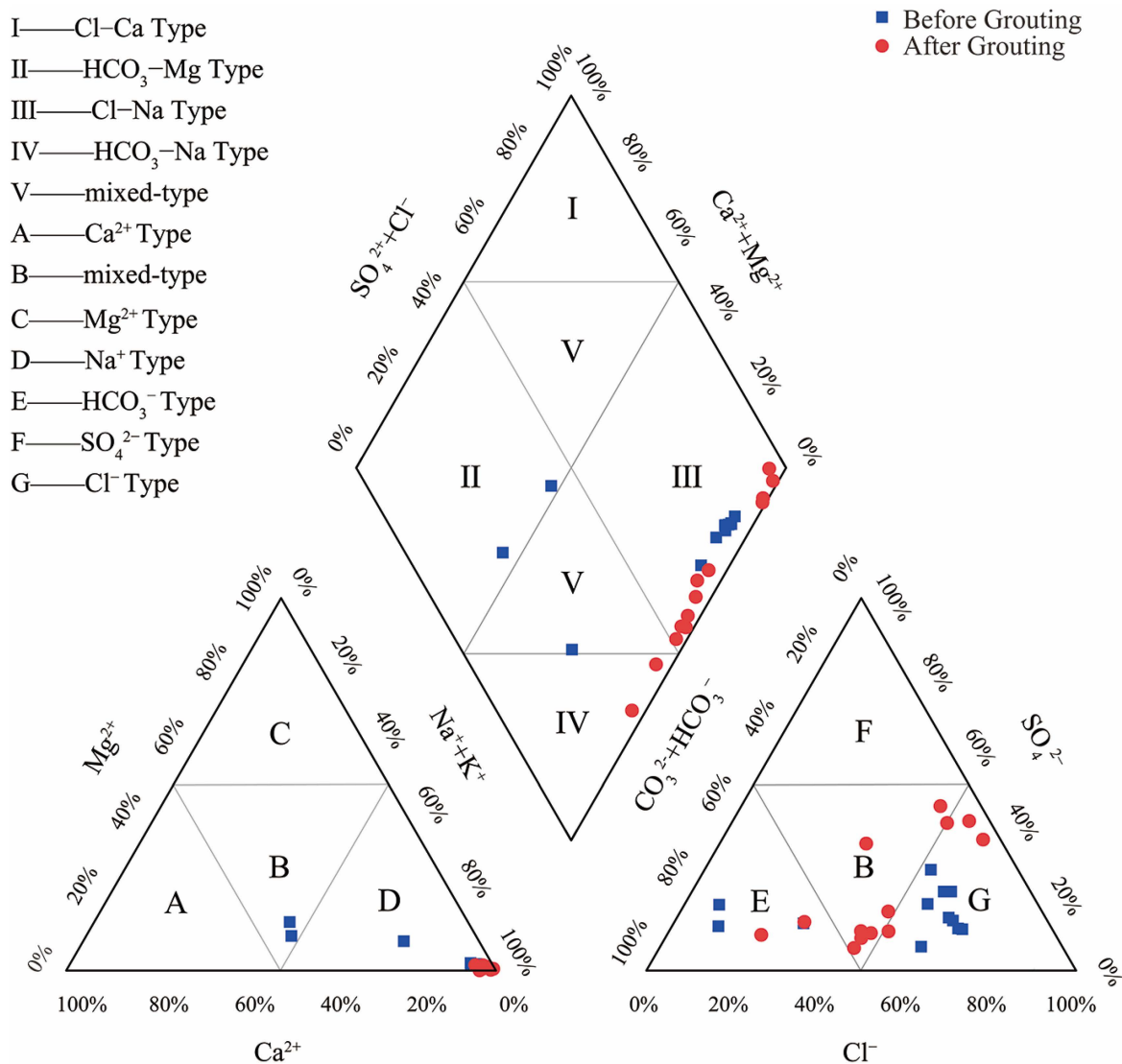


Figure 3. Piper diagram of Taihui water.

Before grouting, Na<sup>+</sup> and Cl<sup>-</sup>, SO<sub>4</sub><sup>2-</sup>, and TDS and Na<sup>+</sup> and Cl<sup>-</sup> and SO<sub>4</sub><sup>2-</sup> have significant positive correlation, the correlation coefficients were 0.746, 0.851, 0.951, 0.764, and 0.816. After grouting, there was a significant correlation between TDS and Na<sup>+</sup>, HCO<sub>3</sub><sup>-</sup>, and SO<sub>4</sub><sup>2-</sup>, which are 0.962 and -0.704. In general, the correlation between the seven indicators after grouting is weakened, and only the correlation between TDS and Na<sup>+</sup> has been good. This may be due to the influence of the separated water from the grouting slurry, which changes the concentration relationship between ions. Before grouting, Na<sup>+</sup> and Ca<sup>2+</sup> are negatively correlated, and Na<sup>+</sup> and Mg<sup>2+</sup> are positively correlated. The situation after grouting is the opposite. This change may be related to the separated water from the grouting slurry and cation exchange.

### 3.4. Ion Combination Ratio

The ion proportional relationship is an important means to infer the hydrogeochemical evolution process of groundwater [37]. When the environment of groundwater changes, the combination ratio between anions and cations will also change. By studying the change trend of the ratio between two or more ions, the formation process of ions in groundwater and the source law of ions can be obtained [38–40]. Through the analysis of Figures 2 and 3, it can be seen that after grouting treatment, the hydrochemical type and ion mass concentration of Taihui water have changed. This change cannot be simply

attributed to the influence of the separated water from the grouting slurry. In order to further understand the hydrochemical evolution process and ion source of Taihui water under the influence of grouting, Figure 4 is drawn.

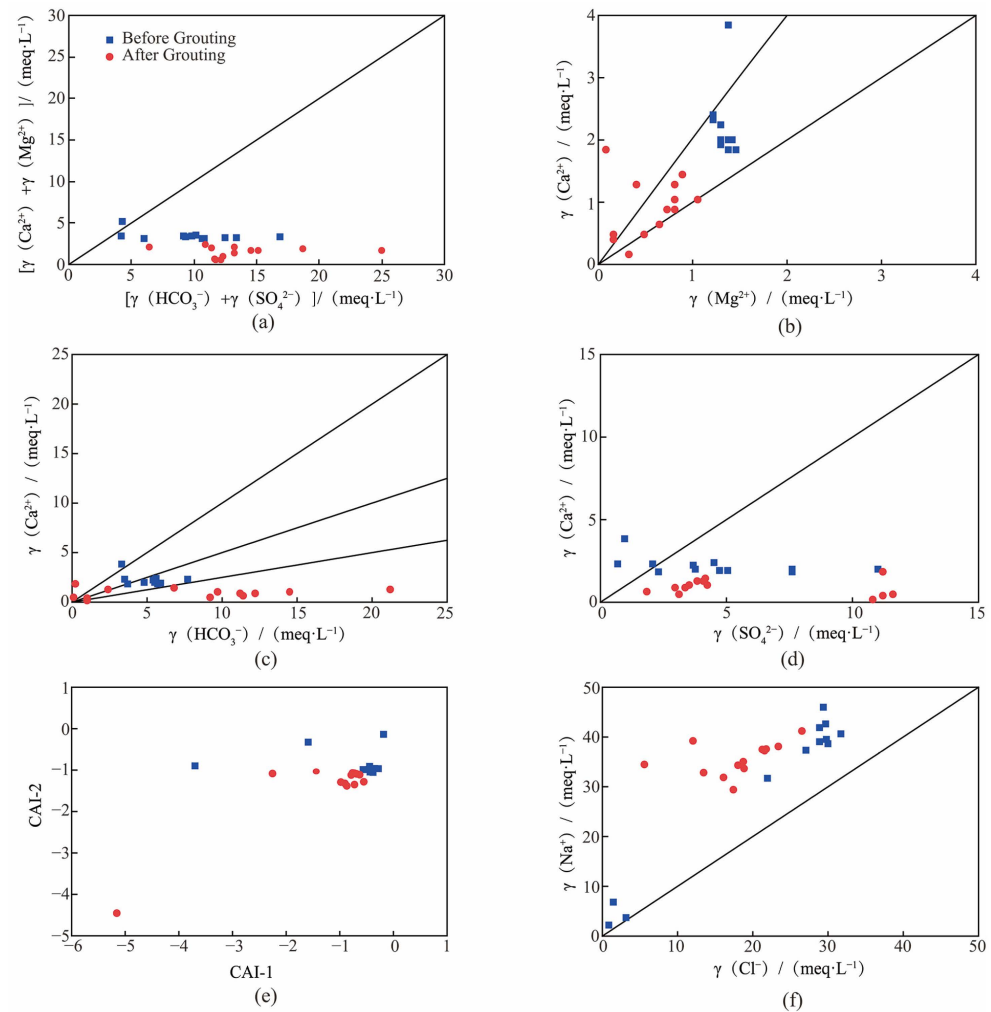


**Figure 4.** Proportional relationship of main ions in Taihui water. (a) The ratio chart of milliequivalent concentrations of  $[\gamma(\text{Ca}^{2+}) + \gamma(\text{Mg}^{2+})]/[\gamma(\text{HCO}_3^-) + \gamma(\text{SO}_4^{2-})]$ ; (b) The ratio chart of milliequivalent concentrations of  $\gamma(\text{Ca}^{2+})/\gamma(\text{Mg}^{2+})$ ; (c) The ratio chart of milliequivalent concentrations of  $\gamma(\text{Ca}^{2+})/\gamma(\text{HCO}_3^-)$ ; (d) The ratio chart of milliequivalent concentrations of  $\gamma(\text{Ca}^{2+})/\gamma(\text{SO}_4^{2-})$ ; (e) The ratio chart between CAI-1 and CAI-2; (f) The ratio chart of milliequivalent concentrations of  $\gamma(\text{Na}^+)/\gamma(\text{Cl}^-)$ .

$[\gamma(\text{Ca}^{2+}) + \gamma(\text{Mg}^{2+})]/[\gamma(\text{HCO}_3^-) + \gamma(\text{SO}_4^{2-})]$  is used to reveal the source of  $\text{Ca}^{2+}$  and  $\text{Mg}^{2+}$  in groundwater. When the ratio is equal to 1, it shows that the  $\text{Ca}^{2+}$  and  $\text{Mg}^{2+}$  in Taihui water are controlled by the dissolution of carbonate and sulfate minerals. When the ratio is greater than 1, it shows that the dissolution of carbonate contributes greatly. When the ratio is less than 1, the main source of  $\text{Ca}^{2+}$  and  $\text{Mg}^{2+}$  is the dissolution of sulfate [41,42]. In Figure 4a, almost all water sample points are below the 1:1 line. Before and after grouting, the main source of  $\text{Ca}^{2+}$  and  $\text{Mg}^{2+}$  in Taihui water is the dissolution of sulfate. Before and after grouting, the average values of  $[\gamma(\text{Ca}^{2+}) + \gamma(\text{Mg}^{2+})]/[\gamma(\text{HCO}_3^-) + \gamma(\text{SO}_4^{2-})]$  are 0.45 and 0.12. After grouting, the dissolution of sulfate is enhanced.

When  $\gamma(\text{Ca}^{2+})/\gamma(\text{Mg}^{2+})$  is equal to 1, it indicates that  $\text{Ca}^{2+}$  and  $\text{Mg}^{2+}$  in Taihui water mainly come from the dissolution of dolomite. When the ratio is greater than 1, it indicates that the dissolution of calcite and dolomite coexists in Taihui water. When the ratio is greater than 2, it shows that in addition to the dissolution of calcite and dolomite, there is

also the dissolution of silicate minerals in Taihui water [43]. In Figure 4b, the water samples before grouting are basically concentrated between the 1:1 line and the 2:1 line.  $\text{Ca}^{2+}$  and  $\text{Mg}^{2+}$  in Taihui water mainly come from the dissolution of calcite and dolomite. One of the water samples (YZ1-1) showed the dissolution of silicate minerals. The water sample points after grouting are dispersed. A total of 30.77% of the water samples were distributed above the 2:1 line, and the remaining 69.23% of the water samples were distributed near the 1:1 line and between the 1:1 line and the 2:1 line. Before and after grouting, the average values of  $\gamma(\text{Ca}^{2+})/\gamma(\text{Mg}^{2+})$  are 1.69 and 3.21. After grouting, the dissolution of calcite and dolomite is enhanced, and the dissolution of silicate minerals exists at some sampling points.

$\gamma(\text{Ca}^{2+})/\gamma(\text{HCO}_3^-)$  is used to reveal the source of  $\text{Ca}^{2+}$  and  $\text{HCO}_3^-$  [44]. In Figure 4c, the water sample points before grouting are mainly distributed near the 1:2 line, indicating that the source is mainly the dissolution of calcite. The water sample points after grouting are mainly distributed near the 1:4 line. In addition to calcite, there is also the leaching effect of dolomite.

$\gamma(\text{Ca}^{2+})/\gamma(\text{SO}_4^{2-})$  is used to reveal the source of  $\text{Ca}^{2+}$  and  $\text{SO}_4^{2-}$ . When the ratio is equal to 1, it indicates that  $\text{Ca}^{2+}$  and  $\text{SO}_4^{2-}$  in groundwater mainly come from gypsum dissolution. When the ratio is greater than 1,  $\text{Ca}^{2+}$  and  $\text{SO}_4^{2-}$  in groundwater mainly come from the dissolution of calcite or dolomite. In Figure 4d, the Taihui water samples after grouting are distributed below the 1:1 line, indicating that in addition to the dissolution of gypsum,  $\text{SO}_4^{2-}$  has other sources, such as the oxidation of pyrite [45,46]. According to the borehole histogram of the study area, pyrite exists in the limestone fissures of C<sub>3</sub>II and C<sub>3</sub>III groups. The oxidation of pyrite will increase the content of  $\text{SO}_4^{2-}$  in Taihui water. Before and after grouting, the average values of  $\gamma(\text{Ca}^{2+})/\gamma(\text{SO}_4^{2-})$  are 1.04 and 0.22. Obviously, the oxidation of pyrite is enhanced after grouting.

The chlor-alkali index is an important index to judge whether there is cation exchange. The calculation formula is as follows:

$$\begin{aligned} \text{CAI} - 1 &= [\gamma(\text{Cl}^-) - \gamma(\text{Na}^+ + \text{K}^+)]/\gamma(\text{Cl}^-) \\ \text{CAI} - 2 &= [\gamma(\text{Cl}^-) - \gamma(\text{Na}^+ + \text{K}^+)]/[\gamma(\text{SO}_4^{2-}) + \gamma(\text{HCO}_3^-)] \end{aligned}$$

When the chlor-alkali index is greater than 0, it shows that  $\text{Na}^+$  in groundwater has cation exchange with  $\text{Ca}^{2+}$  and  $\text{Mg}^{2+}$  in rock. When the chlor-alkali index is greater than 0, it shows that  $\text{Na}^+$  in groundwater has cation exchange with  $\text{Ca}^{2+}$  and  $\text{Mg}^{2+}$  in rock. When the chlor-alkali index is less than 0, it indicates that the cation exchange occurs between  $\text{Ca}^{2+}$  and  $\text{Mg}^{2+}$  in groundwater and  $\text{Na}^+$  in rock [47,48]. The cation exchange reaction equation of water-rock interaction is as follows:

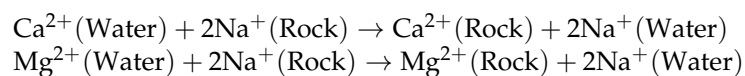


Figure 4e shows that both CAI-1 and CAI-2 are negative. Whether before or after grouting,  $\text{Ca}^{2+}$  and  $\text{Mg}^{2+}$  in Taihui water have cation exchange with  $\text{Na}^+$  in the aquifer minerals, which increases the content of  $\text{Na}^+$  in Taihui water. This rule is also consistent with the data in Table 1. If the absolute value of the chlor-alkali index is larger, the cation exchange is more intense [49]. In this study, the average values of CAI-1 and CAI-2 before grouting are  $-0.75$  and  $-1.27$ . The average values after grouting are  $-0.85$  and  $-1.44$ . By comparing these numbers, it can be seen that the strength of cation exchange after grouting is greater.

$\gamma(\text{Na}^+)/\gamma(\text{Cl}^-)$  is used to reveal the source of  $\text{Na}^+$ . To a certain extent, it reflects the dissolution of salt rock and cation exchange adsorption during water-rock interaction [50,51].  $\text{Cl}^-$  is usually derived from the dissolution of rock salt under hydrodynamic action, which is relatively stable. When the ratio of  $\gamma(\text{Na}^+)/\gamma(\text{Cl}^-)$  is equal to 1, it indicates that  $\text{Na}^+$  mainly comes from the dissolution of rock salt. When the ratio is greater than 1, it indicates that there are other sources of  $\text{Na}^+$  in addition to the dissolution of rock salt. The extra  $\text{Na}^+$  may come from the dissolution of silicate minerals and cation exchange [52]. Figure 4f

shows that the ratios of  $\gamma(\text{Na}^+)/\gamma(\text{Cl}^-)$  are all greater than 1, indicating that they are less affected by the dissolution of rock salt. The enrichment of  $\text{Na}^+$  is mainly due to the dissolution of aluminum silicate or cation exchange in the aquifer. Before grouting, the average value of  $\gamma(\text{Na}^+)/\gamma(\text{Cl}^-)$  is 1.75. After grouting, the average value is 2.22. It shows that silicate minerals dissolution or cation exchange is enhanced after grouting.

According to Table 1 and Figure 2, compared with before grouting, the mass concentration of  $\text{Ca}^{2+}$  and  $\text{Mg}^{2+}$  in Taihui water decreased after grouting. This phenomenon can be explained by three aspects. First, because the fly ash cement contains more  $\text{Ca}^{2+}$  ( $\text{Mg}^{2+}$  is neglected), the separated water from the grouting slurry supplements the rich  $\text{Ca}^{2+}$  for Taihui water. Second, it can be seen from Figure 4a,b that after grouting, the dissolution of sulfate, silicate, calcite, and dolomite is enhanced, thus increasing the content of  $\text{Ca}^{2+}$  and  $\text{Mg}^{2+}$  in Taihui water. Third, although the mass concentration of  $\text{Ca}^{2+}$  and  $\text{Mg}^{2+}$  should increase to a certain extent, the cation exchange after grouting is more intense, so the content of  $\text{Ca}^{2+}$  and  $\text{Mg}^{2+}$  decreases, while the content of  $\text{Na}^+$  increases.

According to Table 1 and Figure 2, the  $\text{Na}^+$  mass concentration of Taihui water in the original environment is high and dispersed, while the average  $\text{Na}^+$  mass concentration after grouting is higher and the data are concentrated. Figure 4e,f can explain this phenomenon. Before grouting, the higher  $\text{Na}^+$  content in limestone water comes from the dissolution of rock salt and cation exchange. After grouting, on the one hand, due to the enhanced dissolution of aluminum silicate, and on the other hand, due to the increase in  $\text{Ca}^{2+}$  and  $\text{Mg}^{2+}$  and the intensification of cation exchange, the average mass concentration of  $\text{Na}^+$  is higher. The coefficient of variation of  $\text{Na}^+$  after grouting is smaller, and it is speculated that the water environment after grouting is more closed, and the reaction is more sufficient.

### 3.5. Saturation Index Analysis

The saturation index (SI) can be used to analyze the equilibrium state between groundwater and aquifer minerals during water–rock interaction [53]. The SI of calcite, dolomite, gypsum, and rock salt is calculated using Phreeqc 3.7.3, and the results are shown in Table 3. If SI is positive, it means that the chemical composition is in a supersaturated state (mineral precipitation). If SI is negative, it means that the chemical composition is in an unsaturated state. That is to say, this mineral will continue to dissolve. Considering the error of calculation, when  $-0.5 < \text{SI} < 0.5$ , the groundwater and aquifer minerals are in equilibrium. It can be seen from Table 3 that the SI of dolomite in four minerals is the largest, followed by calcite, gypsum, and rock salt. Before grouting, the SI of dolomite in Taihui water is 1.12~2.73, with an average of 2.02, indicating that dolomite is almost in a precipitated state. After grouting, the SI of dolomite in Taihui water is  $-1.03$ ~2.60, with an average of 1.23, indicating that most of the dolomite is in a precipitated state. But there are exceptions. The SI of a water sample (YZ3-3) is  $-0.36$ , which indicates that the dolomite is in equilibrium in Taihui water. Another water sample (YZ1-1) has an SI of  $-1.03$ , indicating that dolomite is in a dissolved state. It is possible that the two boreholes are located in the boundary influence zone of the fault and the 2# karst collapse column, and the surrounding strata are relatively broken, and vertical water-conducting fractures have been formed. Therefore, there is an unsaturated area of grouting, so the slurry does not have effective diffusion coverage. Under the influence of vertical water-conducting fissures, dolomite is in a dissolved state. Before grouting, the SI of calcite in Taihui water is 0.64~1.43, with an average of 1.05, indicating that calcite is basically in a precipitated state. After grouting, the SI of calcite in Taihui water is  $-0.32$ ~1.46, with an average value of 0.64. A few are in equilibrium, and most are in precipitation. Before grouting, the SI of gypsum in limestone water is  $-2.23$ ~ $-1.53$ , with an average of  $-1.85$ . After grouting, SI is  $-1.48$ ~ $-2.68$ , with an average of  $-2.21$ . Therefore, the gypsum SI before and after grouting is negative, indicating that the gypsum is almost in a dissolved state. Before grouting, the SI of rock salt in limestone water is  $-7.38$ ~ $-4.63$ , with an average value of  $-5.24$ . After grouting, the SI of rock salt in limestone water is  $-5.43$ ~ $-4.71$ , with an average value of  $-4.96$ . Similarly, this shows that gypsum mostly exists in a dissolved state.

**Table 3.** Saturation index of Taihui water.

	Number	Name	Calcite	Dolomite	Gypsum	Halite
Before	1	SixT-1	1.02	2.01	−1.53	−4.63
	2	SixT-2	1.04	2.08	−1.89	−6.67
	3	SixT-3	1.33	2.56	−1.88	−4.68
	4	SixT-4	1.11	2.15	−1.65	−4.65
	5	SixT-5	1.43	2.73	−2.11	−4.73
	6	SixT-6	1.25	2.48	−1.93	−4.63
	7	SixT-1	1.42	2.69	−1.79	−4.67
	8	SixT-2	0.99	1.66	−1.94	−6.60
	9	SixT-3	0.76	1.47	−1.76	−4.89
	11	SixT-5	0.64	1.12	−2.23	−7.38
	12	SixT-6	0.93	1.81	−1.83	−4.69
		Minimum		0.64	1.12	−2.23
	Mean		1.05	2.02	−1.85	−5.24
	Maximum		1.43	2.73	−1.53	−4.63
After	1	YZ1	0.98	1.87	−1.95	−5.02
	2	YZ1	0.76	1.44	−1.95	−5.43
	3	YZ4-2	0.97	2.08	−2.23	−4.79
	4	YZ4-2	0.79	1.728	−2.68	−4.93
	5	YZ5-1	0.90	1.96	−2.61	−4.94
	6	YZ4-1	0.72	1.53	−2.36	−4.84
	7	YZ3-1	0.65	1.33	−2.11	−5.09
	8	YZ3-1	1.46	2.60	−2.21	−5.07
	9	YZ2-1	0.82	1.70	−2.31	−4.83
	10	YZ3-2	0.48	0.67	−2.12	−5.02
	11	YZ3-2	0.04	0.51	−2.54	−4.92
	12	YZ4-3	−0.32	−0.38	−2.16	−4.86
	13	YZ3-3	0.12	−1.02	−1.48	−4.71
	Minimum		−0.32	−1.03	−2.68	−5.43
	Mean		0.64	1.23	−2.21	−4.96
	Maximum		1.46	2.60	−1.48	−4.71

Compared with the SI before grouting, it is found that the SI of dolomite, calcite, and gypsum is significantly reduced after grouting. According to the previous analysis, this is mainly because the cation exchange makes the content of  $\text{Ca}^{2+}$  and  $\text{Mg}^{2+}$  decreased. On the contrary, the SI of rock salt increased slightly after grouting. This rule is consistent with the change of  $\text{Na}^+$  mass concentration.

#### 4. Conclusions

Through the analysis and comparison of Taihui water samples before and after grouting, the main ion concentration variation characteristics and hydrochemical evolution law of Taihui water under the influence of regional grouting are revealed. The following conclusions were reached:

- (1) There was no change in the order of anion and cation mass concentrations before and after grouting, which are  $\text{Na}^+ + \text{K}^+ > \text{Ca}^{2+} > \text{Mg}^{2+}$  and  $\text{Cl}^- > \text{HCO}_3^- > \text{SO}_4^{2-}$ . However, after grouting, the average values of PH and TDS become larger, the alkalinity of Taihui water is enhanced, and it is medium salinity. In addition, after grouting, the mass concentrations of  $\text{Na}^+ + \text{K}^+$ ,  $\text{Ca}^{2+}$ ,  $\text{Mg}^{2+}$ , and Cl in Taihui water decreased, while the mass concentrations of  $\text{SO}_4^{2-}$  and  $\text{HCO}_3^-$  increased. The separated water of ordinary Portland cement usually leads to the increase in  $\text{Ca}^{2+}$  concentration in Taihui water. However, because the calcium oxide content of fly ash cement is less than that of ordinary Portland cement, and the cation exchange effect is enhanced, the  $\text{Ca}^{2+}$  concentration of Taihui water is reduced. After grouting,

the hydrochemical types of Taihui water are more concentrated, mainly  $\text{HCO}_3\text{-Na}$  and  $\text{Cl-Na}$ .

- (2) The correlation between the conventional indicators of Taihui water is weakened. Through the variation characteristics of main ion concentration, hydrochemical type analysis, and correlation comparison, it is shown that Taihui water is not only directly affected by the separated water from grouting slurry, but also that hydrogeochemical evolution occurs in the limestone aquifer, resulting in significant changes in ion concentration and breaking the original ion balance.  $\text{Ca}^{2+}$ ,  $\text{Mg}^{2+}$ ,  $\text{SO}_4^{2-}$ , and  $\text{HCO}_3^-$  have a high coefficient of variation, that is, these ions are greatly affected.
- (3) The main hydrogeochemical processes in the limestone aquifer are identified by the ion combination ratio, and the source of ions is revealed. Before grouting, the reactions in Taihui water mainly include dissolution (sulfate, carbonate, salt rock, silicate, dolomite, calcite, gypsum), cation exchange, and pyrite oxidation. After grouting, in addition to these effects, there is also the mixing effect of the separated water from the grouting slurry. After grouting, these effects are enhanced. When fly ash cement and ordinary Portland cement are applied to grouting treatment, the main difference between their hydrogeochemical effects on the Taiyuan limestone aquifer is reflected in cation exchange.
- (4) Before and after grouting, dolomite and calcite are almost in a state of precipitation. There are two negative values of dolomite SI after grouting, which is speculated to be due to the influence of faults and the 2# karst collapse column, and there is a slurry-unsaturated area. Therefore, under the influence of vertical water-conducting fissures, dolomite is in a dissolved state. Before and after grouting, gypsum and salt rock are basically in a dissolved state. After grouting, the SI of dolomite, calcite, and gypsum decreased significantly, and the SI of rock salt increased slightly. The law of precipitation or dissolution state of minerals is consistent with the law of mass concentration of conventional ions in Taihui water. Regardless of whether Taihui water is affected by the grouting of fly ash cement or ordinary Portland cement, the variation of mineral saturation index is basically the same.

Based on the above research, Taihui water is greatly affected by grouting engineering with fly ash cement as the material. In the treatment of mine water disasters, the hydrogeochemical evolution law under the influence of grouting should be clarified.

**Author Contributions:** Conceptualization, G.X. and H.L.; methodology, H.L.; validation, G.X. and H.L.; investigation, G.X.; resources, H.L.; writing—original draft preparation, G.X. and H.L.; writing—review and editing, G.X. and H.L.; visualization, G.X.; funding acquisition, H.L. All authors have read and agreed to the published version of the manuscript.

**Funding:** This research was funded by The Open Fund of State Key Laboratory of Coal Resources and Safe Mining, grant number SKICRSM23KFA06, the National Key Research and Development Program of China, grant number 2022YFF1303302, the National Natural Science Foundation of China, grant number 41977253, and the Graduate Student Innovation Fund of Anhui University of Science and Technology, grant number 2023cx2007.

**Data Availability Statement:** The data used in this paper can be accessed by contacting the corresponding author directly.

**Conflicts of Interest:** The authors declare no conflicts of interest.

## References

1. Wu, Q. Progress, problems and prospects of prevention and control technology of mine water and reutilization in China. *J. China Coal Soc.* **2014**, *39*, 795–805.
2. Zeng, Y.F.; Wu, Q.; Zhao, S.Q.; Miao, Y.W.; Zhang, Y.; Mei, A.S.; Meng, S.H.; Liu, X.X. Characteristics, causes, and prevention measures of coal mine water hazard accidents in China. *Coal Sci. Technol.* **2023**, *51*, 1–14.
3. Dong, S.N.; Guo, X.M.; Liu, Q.S.; Wang, H.; Nan, S.H.; Zheng, S.T.; Wang, Y.H. Model and selection criterion of zonal preact grouting to prevent mine water disasters of coal floor limestone aquifer in North China type coalfield. *Coal Geol. Explor.* **2020**, *48*, 1–10.

4. Zheng, S.T. Advanced exploration and control technology of limestone water hazard in coal seam floor in Huainan and Huaibei coalfields. *Coal Geol. Explor.* **2018**, *46*, 142–146+153.
5. Guo, Y.; Gui, H.R.; Wei, J.C.; Pang, Y.C.; Hu, M.C.; Guo, X.D.; Hong, H.; Nie, F.; Cui, Y.L.; Ye, S. Hydrogeochemical evolution law of Taiyuan Formation limestone water under coal seam floor caused by the influence of regional grouting. *J. China Coal Soc.* **2023**, *48*, 3204–3217.
6. Ramanathan, S.; Gopinath, S.C.B.; Arshad, M.K.M.; Poopalan, P. Nanostructured aluminosilicate from fly ash: Potential approach in waste utilization for industrial and medical applications. *J. Clean. Prod.* **2020**, *253*, 119923. [[CrossRef](#)]
7. Piper, A.M. A graphic procedure in the geochemical interpretation of water-analyses. *Trans. Am. Geophys. Union* **1944**, *25*, 914–928. [[CrossRef](#)]
8. Zhao, D.; Zeng, Y.F.; Wu, Q.; Du, X.; Gao, S.; Mei, A.S.; Zhao, H.N.; Zhang, Z.H.; Zhang, X.H. Source discrimination of mine gushing water using self-organizing feature maps: A case study in Ningtiaota Coal Mine, Shaanxi, China. *Sustainability* **2022**, *14*, 6551. [[CrossRef](#)]
9. Durov, S.A. Natural waters and graphic representation of their composition. *Dokl. Akad. Nauk. SSSR* **1948**, *59*, 87–90.
10. Reddy, A.G.S.; Kumar, K.N. Identification of the hydrogeochemical processes in groundwater using major ion chemistry: A case study of Penna-Chitravathi river basins in Southern India. *Environ. Monit. Assess.* **2010**, *170*, 365–382. [[CrossRef](#)] [[PubMed](#)]
11. Patil, S.; Patil, B.; Kadam, A.; Wagh, V.; Patil, A.; Pimparkar, A.; Karuppannan, S.; Sahu, U. Nitrate and fluoride contamination in the groundwater in a tribal region of north Maharashtra, India: An account of health risks and anthropogenic influence. *Groundw. Sustain. Dev.* **2024**, *25*, 101107. [[CrossRef](#)]
12. Wagh, V.; Mukate, S.; Muley, A.; Kadam, A.; Panaskar, D.; Varade, A. Study of groundwater contamination and drinking suitability in basaltic terrain of Maharashtra, India through PIG and multivariate statistical techniques. *J. Water Supply Res. Technol. Aqua* **2020**, *69*, 398–414. [[CrossRef](#)]
13. Srivastava, M.; Srivastava, P.K.; Kumar, D.; Kumar, A. A systematic study of uranium in groundwater and its correlation with other water quality parameters. *Water Supply* **2022**, *22*, 2478–2492. [[CrossRef](#)]
14. Krishan, G.; Bhagwat, A.; Sejwal, P.; Yadav, B.K.; Kansal, M.L.; Bradley, A.; Singh, S.; Kumar, M.; Sharma, L.M.; Muste, M. Assessment of groundwater salinity using principal component analysis (PCA): A case study from Mewat (Nuh), Haryana, India. *Environ. Monit. Assess.* **2023**, *195*, 37. [[CrossRef](#)] [[PubMed](#)]
15. Qin, W.J.; Song, X.F.; Gu, H.B. Impacts of the Liujiang Coal Mine on groundwater quality based on hierarchical cluster analysis. *Hydrogeol. Eng. Geol.* **2018**, *45*, 30–39.
16. Wagh, V.M.; Panaskar, D.B.; Jacobs, J.A.; Mukate, S.V.; Muley, A.A.; Kadam, A.K. Influence of hydro-geochemical processes on groundwater quality through geostatistical techniques in Kadava River basin, Western India. *Arab. J. Geosci.* **2019**, *12*, 7. [[CrossRef](#)]
17. Mukate, S.; Panaskar, D.; Wagh, V.; Muley, A.; Jangam, C.; Pawar, R. Impact of anthropogenic inputs on water quality in Chincholi industrial area of Solapur, Maharashtra, India. *Groundw. Sustain. Dev.* **2018**, *7*, 359–371. [[CrossRef](#)]
18. Zhou, C.C.; Liu, G.J.; Fang, T.; Sun, R.Y.; Wu, D. Leaching characteristic and environmental implication of rejection rocks from Huainan Coalfield, Anhui Province, China. *J. Geochem. Explor.* **2014**, *143*, 54–61. [[CrossRef](#)]
19. Xu, G.Q.; Zhang, H.T.; Zhou, J.S.; Li, X.; Wang, M.H.; Liu, M.C. Study and prospect of karst collapse columns and their water inrush in the coalfield of North China. *Carsologica Sin.* **2022**, *41*, 259–275.
20. Zheng, S.T.; Ma, P.Z. The technique building “concrete plug” quickly in collapse column. *Coal Geol. Explor.* **1998**, *3*, 52–54.
21. Bi, B.; Chen, Y.C.; Xie, H.; An, S.K.; Xu, Y.F. Water inrush warning system of deep limestone in Panxie Mining Area based on multi-source data mining. *J. China Coal Soc.* **2022**, *50*, 81–88.
22. Qin, Y.; Lu, J. Prediction of coal mine water hazards: A case study from the Huainan Coalfield. *Arab. J. Geosci.* **2019**, *12*, 83. [[CrossRef](#)]
23. Jiang, Q.L.; Liu, Q.M.; Liu, Y.; Chai, H.C.; Zhu, J.Z. Groundwater chemical characteristic analysis and water source identification model study in Gubei coal mine, Northern Anhui Province, China. *Heliyon* **2024**, *10*, e26925. [[CrossRef](#)] [[PubMed](#)]
24. Zhang, H.T.; Xu, G.Q.; Chen, X.Q.; Wei, J.; Yu, S.T.; Yang, T.T. Hydrogeochemical Characteristics and Groundwater Inrush Source Identification for a Multi-aquifer System in a Coal Mine. *Acta Geol. Sin.* **2019**, *93*, 1922–1932. [[CrossRef](#)]
25. Xue, J.J.; Ma, L.; Qian, J.Z.; Zhao, W.D. Hydrogeochemical characteristics and evolution mechanism of groundwater in the Guqiao Coal Mine, Huainan Coalfield, China. *Environ. Earth Sci.* **2024**, *83*, 35. [[CrossRef](#)]
26. An, S.K.; Jiang, C.L.; Zhang, W.X.; Chen, X.; Zheng, L.G. Influencing factors of the hydrochemical characteristics of surface water and shallow groundwater in the subsidence area of the Huainan Coalfield. *Arab. J. Geosci.* **2020**, *13*, 191. [[CrossRef](#)]
27. Ma, L.; Qian, J.Z.; Zhao, W.D.; Zhou, X.P. Multivariate statistical analysis of chemical characteristics of groundwater in Gubei Coal Mine. *J. China Coal Soc.* **2013**, *26*, 1495–1498+1503.
28. Yang, T.T.; Xu, G.Q.; Yu, S.T.; Su, Y.; Zheng, Z.Y.; Li, Z.H. An analysis of the chemical composition characteristics and formation of the karst groundwater in the Taiyuan Group in the lower part of a coal seam. *Hydrogeol. Eng. Geol.* **2019**, *46*, 100–108.
29. Zheng, Z.Y.; Xu, G.Q.; Yang, T.T.; Yu, S.T.; Zhang, H.T. Hydrochemical formation mechanism and transmissivity-impermeability analysis of karst groundwater on both sides of fault F<sub>104</sub> in Gubei coal mine in Huainan. *Coal Geol. Explor.* **2020**, *48*, 129–137.
30. Dong, F.Y.; Yin, H.Y.; Cheng, W.J.; Li, Y.J.; Qiu, M.; Zhang, C.W.; Tang, R.Q.; Xu, G.L.; Zhang, L.F. Study on water inrush pattern of Ordovician limestone in North China Coalfield based on hydrochemical characteristics and evolution processes: A case study in Binhu and Wangchao Coal Mine of Shandong Province, China. *J. Clean. Prod.* **2022**, *380*, 134954. [[CrossRef](#)]

31. Chen, K.; Liu, Q.M.; Liu, Y.; Peng, W.H.; Wang, Z.T.; Zhao, X. Hydrochemical characteristics and source analysis of deep groundwater in Qianyingzi Coal Mine. *Coal Geol. Explor.* **2022**, *50*, 99–106.
32. Ju, Q.D.; Liu, Y.; Hu, Y.B.; Wang, Y.Q.; Liu, Q.M.; Wang, Z.T. Hydrogeochemical evolution and control mechanism of underground multiaquifer system in coal mine area. *Geofluids* **2020**, *2020*, 8820650. [[CrossRef](#)]
33. Guo, Q.L.; Yang, Y.S.; Han, Y.Y.; Li, J.L.; Wang, X.Y. Assessment of surface-groundwater interactions using hydrochemical and isotopic techniques in a coalmine watershed, NW China. *Environ. Earth Sci.* **2019**, *78*, 91. [[CrossRef](#)]
34. Li, Y.A.; Wang, Q.Q.; Jiang, C.L.; Li, C.; Hu, M.Y.; Xia, X. Spatial characteristics and controlling indicators of major hydrochemical ions in rivers within coal-grain composite areas via multivariate statistical and isotope analysis methods. *Ecol. Indic.* **2024**, *158*, 111352. [[CrossRef](#)]
35. Liu, Q.H.; Wu, B.; Wu, G.; Gao, F.; Du, M.L.; Cao, W. Evolution and mechanism analysis of groundwater chemical characteristics in the context of overexploitation—A case study of Qitai County, eastern part of Changji Prefecture, Xinjiang. *Acta Sci. Circumstantiae* **2023**. [[CrossRef](#)]
36. Wei, S.M.; Ding, G.T.; Yuan, G.X.; Wang, L.F.; Nie, Y.P.; Du, J.L. Hydrochemical characteristics and formation mechanism of groundwater in Yí'nan, East Wenhe River basin in Shangdong Province. *Acta Geol. Sin.* **2021**, *95*, 1973–1983.
37. Bian, C.; Lv, Y.G.; Zhang, H.S.; Liu, J.W.; Feng, C.X.; Chen, T.; Zhao, M.; Cai, W.T. Hydrochemical characteristics and variation of karst groundwater in the Baiquan Spring area of Xingtai over the last 30 years. *Environ. Sci.* **2024**. [[CrossRef](#)]
38. Chen, L.W.; Xu, D.Q.; Yin, X.X.; Xie, W.P.; Zeng, W. Analysis on hydrochemistry and its control factors in the concealed coal mining area in North China: A case study of dominant inrush aquifers in Suxian mining area. *J. China Coal Soc.* **2017**, *42*, 996–1004.
39. Guo, Y.N.; Li, G.Q.; Wang, L.; Zhang, Z. Hydrochemical Characteristics of Mine Water and Their Significance for the Site Selection of an Underground Reservoir in the Shendong Coal Mining Area. *Water* **2023**, *15*, 1038. [[CrossRef](#)]
40. Guo, Y.; Gui, H.R.; Wei, J.C.; Pang, Y.C.; Hu, M.C.; Zhang, Z.; Nie, F.; Hong, H.; Cui, Y.L.; Zhao, J. Hydrogeochemical evolution of Taiyuan formation limestone water under the disturbance of water inrush from karst collapse column in Taoyuan coal mine, China. *Water Supply* **2022**, *22*, 8196–8210. [[CrossRef](#)]
41. Kumar, P.; Singh, A.K. Hydrogeochemistry and quality assessment of surface and sub-surface water resources in Raniganj coalfield area, Damodar Valley, India. *Int. J. Environ. Anal. Chem.* **2022**, *102*, 8346–8369. [[CrossRef](#)]
42. Liu, P.; Yang, M.; Sun, Y.J. Hydro-geochemical processes of the deep Ordovician groundwater in a coal mining area, Xuzhou, China. *Hydrogeol. J.* **2019**, *27*, 2231–2244. [[CrossRef](#)]
43. Qian, J.Z.; Wang, L.; Ma, L.; Lu, Y.H.; Zhao, W.D.; Zhang, Y. Multivariate statistical analysis of water chemistry in evaluating groundwater geochemical evolution and aquifer connectivity near a large coal mine, Anhui, China. *Environ. Earth Sci.* **2016**, *75*, 747. [[CrossRef](#)]
44. Sun, F.Y. Study on Hydrochemical Characteristics and Formation Mechanism of Karst Groundwater in Huainan Coalfield. Master's Thesis, Anhui University of Science and Technology, Huainan, China, 2022.
45. Wang, C.Y.; Liao, F.; Wang, G.C.; Qu, S.; Mao, H.R.; Bai, Y.F. Hydrogeochemical evolution induced by long-term mining activities in a multi-aquifer system in the mining area. *Sci. Total Environ.* **2023**, *854*, 158806. [[CrossRef](#)] [[PubMed](#)]
46. Chen, L.W.; Zheng, X.; Zhang, J.; Zhang, M.; Hu, Y.S.; Zheng, J.; Yin, X.X. Study on the spatial evolution mechanism of hydrochemistry in bedrock aquifer of concealed coal mine based on quantification evaluation of fault. *Acta Geol. Sin.* **2023**, *4*, 23033. [[CrossRef](#)]
47. Zhou, Z.Q.; Huang, Q.B.; Wang, Y.S.; Luo, F.; Liang, J.H.; Xiong, J.Y. Recharge sources and hydrochemical evolution mechanism of surface water and groundwater in typical karst mining area. *Environ. Sci.* **2024**. [[CrossRef](#)]
48. Sun, K.; Fan, L.M.; Ma, W.C.; Chen, J.P.; Peng, J.; Zhang, P.H.; Gao, S.; Li, C.; Miao, Y.P.; Wang, H.K. Geochemical characteristics of groundwater about Zhiluo Formation in the northern Ordos Basin and its indicative significance. *J. China Coal Soc.* **2023**, *2*. [[CrossRef](#)]
49. Han, S.B.; Zhou, Y.Z.; Zheng, Y.; Zhou, J.L.; Li, C.Q.; Han, Q.Q.; Li, F.C. Formation Mechanism and Source Apportionment of Hydrochemical Components in Groundwater in the Yinchuan Plain. *Environ. Sci.* **2023**. [[CrossRef](#)]
50. Han, Y.; Wang, G.C.; Cravotta, C.A.; Hu, W.Y.; Bian, Y.Y.; Zhang, Z.W.; Liu, Y.Y. Hydrogeochemical evolution of Ordovician limestone groundwater in Yanzhou, North China. *Hydrol. Processes* **2012**, *27*, 2247–2257. [[CrossRef](#)]
51. Zhang, J.; Chen, L.W.; Hou, X.W.; Ren, X.X.; Li, J.; Chen, Y.F. Hydrogeochemical processes of carboniferous limestone groundwater in the Yangzhuang Coal Mine, Huaibei Coalfield, China. *Mine Water Environ.* **2022**, *41*, 504–517. [[CrossRef](#)]
52. Murkute, Y.A. Hydrogeochemical characterization and quality assessment of groundwater around Umrer coal mine area Nagpur District, Maharashtra, India. *Environ. Earth Sci.* **2014**, *72*, 4059–4073. [[CrossRef](#)]
53. Okofo, L.B.; Bedu-Addo, K.; Martienssen, M. Characterization of groundwater in the 'Tamnean' Plutonic Suite aquifers using hydrogeochemical and multivariate statistical evidence: A study in the Garu-Tempene District, Upper East Region of Ghana. *Appl. Water Sci.* **2022**, *12*, 22. [[CrossRef](#)]

**Disclaimer/Publisher's Note:** The statements, opinions and data contained in all publications are solely those of the individual author(s) and contributor(s) and not of MDPI and/or the editor(s). MDPI and/or the editor(s) disclaim responsibility for any injury to people or property resulting from any ideas, methods, instructions or products referred to in the content.